DOI: 10.1002/ejic.200800032

A Tetragonal Core with Asymmetric Iron Environments Supported Solely by Bis(μ-OH){μ-(O–H···O)} Bridging and Terminal Pyridine Amide (N, O) Coordination: A New Member of the Tetrairon(III) Family

Akhilesh K. Singh,[a] Wilson Jacob,[a] Athanassios K. Boudalis,[b][‡] Jean-Pierre Tuchagues,[b] and Rabindranath Mukherjee*[a]

Keywords: Iron / Hydroxido bridges / Pyridine amide ligands / Magnetism / Mössbauer spectroscopy

Room-temperature aerobic reaction of $[Fe(MeCN)_4][ClO_4]_2$ with 1,3-bis(2-pyridinecarboxamido)propane (H_2bpp) yields the tetrairon(III) complex $[Fe_4(H_2bpp)_4(\mu\text{-}OH)_2(\mu\text{-}OHO)][ClO_4]_7\cdot 2H_2O\cdot x$MeCN (**1**·x MeCN, $0 \le x \le 3$). Crystal structure determination reveals that **1**·3MeCN is a new member of the tetrairon(III) family, bridged solely by two hydroxido ligands and a localized $\{O\text{–}H\cdots O\}^{3-}$ bridging unit. The properties of the "tetragonal" core $[Fe_4(\mu\text{-}OH)_2\{\mu\text{-}(O\text{–}H\cdots O)\}]^{7+}$ have been investigated by variable-temperature magnetic and Mössbauer spectroscopic measurements. Successful modeling of the data has revealed asymmetric iron environments and three types of magnetic exchange interactions [through μ-OH and μ-O/μ-OH of μ-(O–H···O) bridges]. This tetragonal core is a valuable addition to the tetrairon(III) cluster family from inorganic and bioinorganic perspectives.

Introduction

There has been continued interest in the development of the coordination chemistry of peptide ligands containing the pyridine-2-carboxamide[1–5] and pyridine-2,6-dicarboxamide[1,6–8] functionality in their deprotonated form. Many such complexes act as bioinorganic models[9] and catalysts for selective organic transformations.[4i,4j,10] From the standpoint of exploring the coordination chemistry of deprotonated pyridine amide ligands, we[2,6] and others[3–5,7,8] have synthesized, structurally characterized, and investigated properties of a large variety of interesting transition-metal complexes.

In our efforts to synthesize dinuclear/polynuclear complexes of iron(III), taking into account the oxophilicity of iron(III), we directed our attention to a potentially tetradentate pyridine amide ligand, 1,3-bis(2-pyridinecarboxamido)propane (H_2bpp)[11,12] (Scheme 1), which is capable of providing pyridine N and amide O donor atoms in its neutral form.[12a–12c,13] Due to chelate-ring flexibility, it is interesting to note here the structural diversity of H_2bpp-coordinated transition-metal complexes (Scheme 2).[12a–12c] In Scheme 2, the coordination ability of bpp^{2-} is also included.[12d] We reasoned that initial reaction between equimolar $[Fe^{II}(CH_3CN)_4][ClO_4]_2$[14] and H_2bpp would provide coordination to at least two metal ions due to two pyridine amide moieties present in a H_2bpp ligand and that such a coordination would trigger in each metal ion a search for additional coordination. This in turn would initiate nucleation of a dinuclear/polynuclear species utilizing oxide/hydroxide ions, formed as a result of the reduction of dioxygen with concomitant oxidation of iron(II). The present contribution is the outcome of such an endeavor. Herein we report our results on the synthesis and structural characterization of a tetrairon(III) complex $[(H_2bpp)_4Fe_4(\mu\text{-}OH)_2(\mu\text{-}OHO)][ClO_4]_7\cdot 2H_2O\cdot x$MeCN (**1**·x MeCN, $0 \le x \le 3$; crystal structure: **1**·3MeCN) with a "tetragonal" $\{Fe^{III}_4(\mu\text{-}OH)_2(\mu\text{-}OHO)\}^{7+}$ core (see below). This compound exhibits an aesthetically pleasing structure, distinct from other examples,[15] and also exhibits notable magnetic and Mössbauer

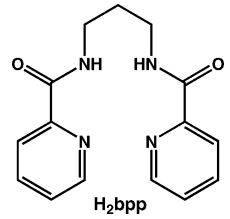

Scheme 1. The 1,3-bis(2-pyridinecarboxamido)propane (H_2bpp) ligand.

[a] Department of Chemistry, Indian Institute of Technology Kanpur,
Kanpur 208016, India
Fax: +91-512-2597436
E-mail: rnm@iitk.ac.in
[b] Laboratoire de Chimie de Coordination, UPR 8241, CNRS, 31077 Toulouse, Cedex 04, France
[‡] Present address: Institute of Materials Science, NCSR "Demokritos"
15310 Aghia Paraskevi Attikis, Greece

Supporting information for this article is available on the WWW under http://www.eurjic.org or from the author.

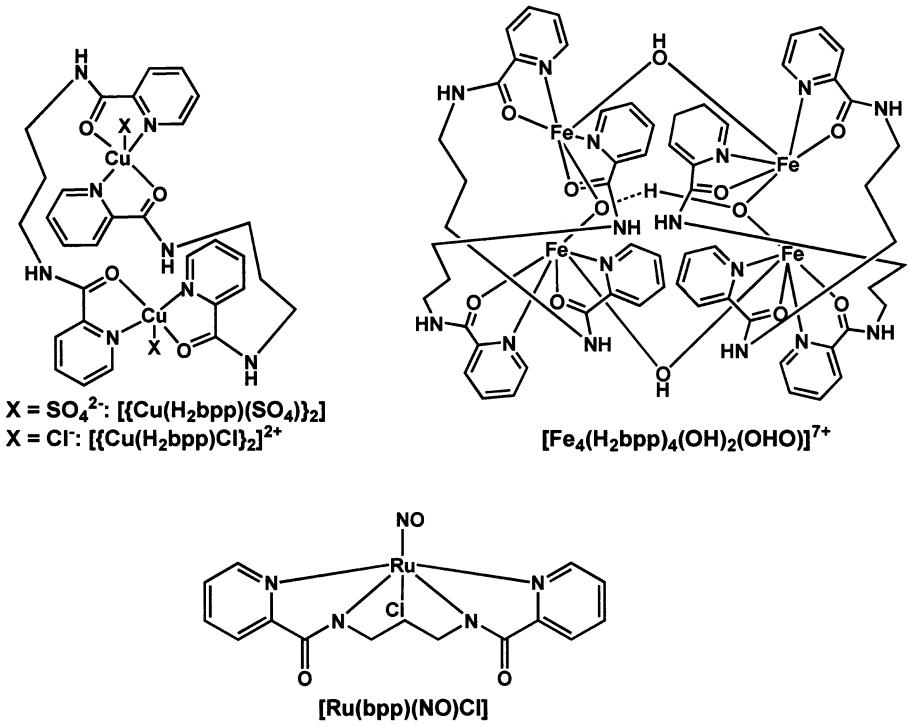

Scheme 2. Structurally verified coordination modes of H_2bpp and bpp^{2-} reported so far. The one observed in this work is also included.

behavior. It is appropriate to mention here that a considerable number of discrete tetrairon(III) complexes have been synthesized and spectroscopically and structurally characterized.[15–17] Notably, all known Fe_4O_4 cores (charges are disregarded), which are either of the dimer-of-dimer type, e.g. [{Fe_2(OR)(RCO_2)}$_2$($O)_2$],[16] or of the tetragonal type, e.g. [{Fe_2(OR)(OCO_2)}$_2$(OHO)],[15a] [{Fe_2(OR)(RCO_2)}$_2$(OHO)],[15b–15e] [{Fe_2(OR)}$_2$(RCO_2)(OHO)],[15e] [{Fe_2(OR)}$_2$(OHO)],[15e,15f] [{Fe_2(OH)($RCO_2)_2$}$_2$(OHO)][15g,15h] (OR^-: alkoxido) and [{Fe_2(OR′)(RCO_2)}$_2$(OHO)][15i] (OR′$^-$: phenoxido) have been assembled by using (i) endogenous alkoxido/phenoxido bridging ligands with or without additional carboxylate bridges and (ii) carboxylate bridges.

Results and Discussion

Synthesis and General Characterization

The synthesis of the title compound is based on the following considerations: (i) H_2bpp is a potentially tetradentate ligand in its deprotonated form.[12d] (ii) H_2bpp can hold two metal ions, each utilizing a 2-pyridinecarboxamide moiety in its neutral form (Scheme 2).[12a–12c,13] Notably, in such a situation the ligand can afford discrete or polymeric compounds containing at least two metal ions. (iii) Aerobic reaction between an iron(III) salt, H_2bpp, and a base could give rise to an intractable polymeric material.[18] Keeping these points in mind, we directed our attention to the aerobic reaction between [Fe(MeCN)$_4$][ClO_4]$_2$ and H_2bpp in a 1:1 molar ratio in MeCN. This led to the formation and isolation of the complex [Fe_4(H_2bpp)$_4$(μ-$OH)_2$(μ-OHO)][-ClO_4]$_7$·2H_2O·*x*MeCN (**1**·*x*MeCN). The formation of **1** could be rationalized by the stoichiometric reaction shown in Equation (1).

$$4[Fe^{II}(MeCN)_4][ClO_4]_2 + 4H_2bpp + O_2 + 2H_2O \rightarrow [Fe^{III}{}_4(H_2bpp)_4\text{-}(\mu\text{-}OH)_2(\mu\text{-}OHO)][ClO_4]_7 + HClO_4 + 16MeCN \quad (1)$$

It is reasonable to assume that the source of OH^- and $\{O–H\cdots O\}^{3-}$ ions is the trace amount of H_2O present in MeCN. The ligand coordinates in its neutral form, as evidenced by the ν(NH) vibration in its IR spectrum. The existence of OH^- and $\{O–H\cdots O\}^{3-}$ is supported by IR spectroscopy [two medium broad bands at ca. 3580 and 3070 cm^{-1} (Figure S1, Supporting Information) due to the O–H stretching mode of the bridging OH^-/solvent of crystallization and $\{O–H\cdots O\}^{3-}$ groups, respectively].[15g,15h] Single-crystal X-ray crystallography authenticated the composition of compound **1** (see below). Orange MeCN/MeOH solutions of **1** display strong OH^-/$\{O–H\cdots O\}^{3-}$ → Fe^{III} charge-transfer transitions at 360/330 nm (Figure S2, Supporting Information).

Crystal Structure of [Fe_4(H_2bpp)$_4$(μ-$OH)_2$(μ-OHO)]-[ClO_4]$_7$·2H_2O·3MeCN (1·3MeCN)

Compound **1**·3MeCN crystallizes in the noncentrosymmetric orthorhombic space group *Fdd*2, and hence it does not have a crystallographically imposed symmetry. Compound **1** consists of a cationic tetrairon species, seven perchlorate counteranions, two H_2O and three MeCN solvate molecules. Given the crystallographically established pres-

ence of seven perchlorate ions and the fact that the four metal centers are clearly Fe^{III} atoms, charge considerations require that three core oxygen atoms be formally protonated (see below). The molecular structure of the heptacation depicts (Figure 1) a novel $\{Fe^{III}_4(\mu\text{-}OH)_2(\mu\text{-}OHO)\}^{7+}$ core assembled solely by four terminally coordinated H_2bpp ligands and bridged by two hydroxide ions and a $\{O\text{–}H\cdots O\}^{3-}$ bridging unit (see below). Each H_2bpp ligand provides a pyridyl N and an amido O to two Fe^{III} ions. As a consequence, each Fe^{III} center has an N_2O_4 donor set in a distorted octahedral geometry (Table 1). The two bridging angles, Fe(1)–O(12)–Fe(4) and Fe(2)–O(10)–Fe(3), are 132.8(3) and 133.0(3)°, respectively. On the basis of this information, we can assign the bridges between Fe(1)/Fe(4) and Fe(2)/Fe(3) as hydroxido ligands. The Fe–O distances Fe(1)–O(12), Fe(4)–O(12), Fe(2)–O(10), and Fe(3)–O(10) [1.942(6)–1.980(6) Å] in the Fe(1)–O(12)–Fe(4) and Fe(2)–O(10)–Fe(3) units fall within the range reported (1.93–1.98 Å) for complexes containing the $\{Fe_2(\mu\text{-}OH)(\mu\text{-}O_2CR)_2\}^{2+}$ unit.[19,20] Notably, the two other bridging angles, Fe(1)–O(9)–Fe(2) and Fe(3)–O(11)–Fe(4), are 149.2(4) and 150.3(4)°, respectively.

It is worth mentioning here that the hydrogen atoms of the bridging units as well as those of the two water molecules present in the crystal lattice of **1**·3MeCN were not located from difference Fourier maps. However, the following observations are noteworthy. The Fe(1)–O(9), Fe(2)–O(9), Fe(3)–O(11), and Fe(4)–O(11) bond lengths are in the range 1.841(6)–1.882(6) Å. They are significantly longer than those of μ-oxido diiron(III) complexes (1.76–1.82 Å), including complexes containing the $\{Fe_2(\mu\text{-}O)(\mu\text{-}O_2CR)_2\}^{2+}$ unit,[20–23] but shorter than Fe^{III}–(μ-OH) distances (1.93–1.98 Å; see above). Thus, the "hydroxido" and "oxido" ligands of the $\{O\text{–}H\cdots O\}^{3-}$ unit can be distinguished on the basis of the Fe–O bond lengths. Moreover, the O···O distances between O(9) and O(11) and between O(10) and O(12) are 2.4874(2) and 4.9854(17) Å, respectively (Figure 1). The former distance indicates the presence of a strong hydrogen bond.[15g–15i,24,25] The possibility exists that oxygen atoms O(9) and O(11) are differently protonated,[15e] as evidenced by their bond lengths to Fe^{III} atoms [Fe–O(9): 1.841(6) and 1.858(6) Å; Fe–O(11): 1.873(6) and 1.882(6) Å] (Table 1). Differences in Fe–O(H) distances of similar magnitude due to localized O–H···O hydrogen bonding were observed before for Fe_4 complexes with endogenous alkoxido/phenoxido bridging ligands with[15i] and without[15e] additional carboxylate bridges. Considering the facts mentioned above, we are inclined to believe that the Fe(1)···Fe(2) and Fe(3)···Fe(4) bridges are provided by the $\{O\text{–}H\cdots O\}^{3-}$ unit and that the proton is bound to O(11). The calculated O(11)–H and O(9)–H distances are 0.95 and 1.543(1) Å, respectively. Similar distances are known for O–H···O hydrogen-bonding interactions.[15c,15d,15f–15h,17] It is interesting to note that the O(9)···O(11) distance is slightly longer than those observed for similar $\{O\cdots H\cdots O\}^{3-}$ bridging units (2.394–2.426 Å)[15a–15d] but shorter than that reported for the rectangular $\{Fe^{III}_4(\mu\text{-}OH)_2(\mu\text{-}OHO)\}^{7+}$ core supported by additional acetate bridges [2.525(9) Å][15g,15h]

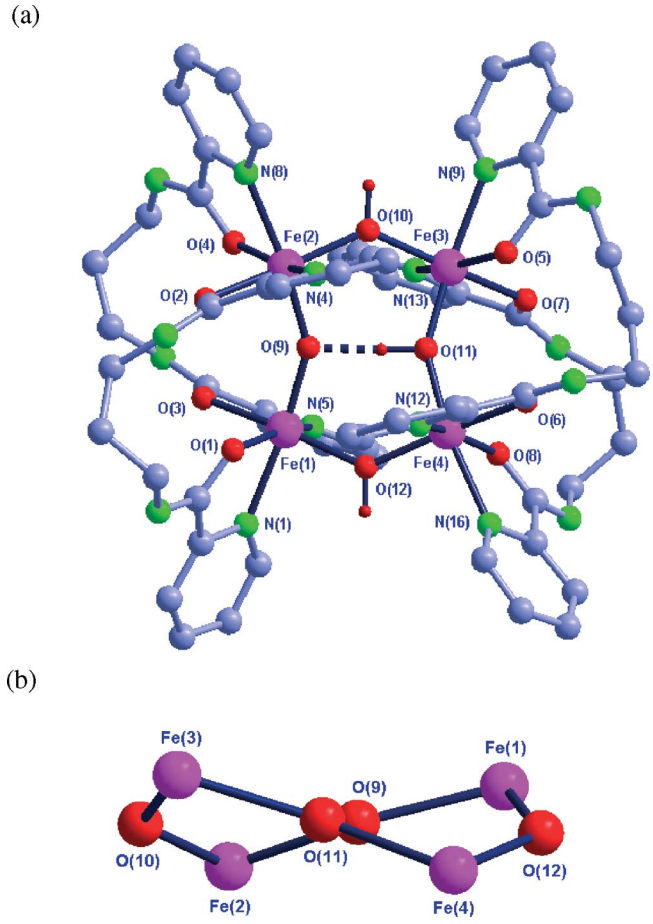

Figure 1. (a) A perspective view of the heptacation $[Fe_4(H_2bpp)_4(\mu\text{-}OH)_2\{\mu\text{-}(O\cdots H\text{–}O)\}]^{7+}$ of $[Fe_4(H_2bpp)_4(\mu\text{-}OH)_2(\mu\text{-}OHO)][ClO_4]_7\cdot 2H_2O\cdot 3MeCN$ (**1**·3MeCN). The hydrogen atoms are omitted for clarity. (b) A view of connectivities within the $Fe^{III}_4O_4$ core.

Table 1. Selected bond lengths [Å] and bond angles [°] for $[Fe_4(H_2bpp)_4(\mu\text{-}OH)_2(\mu\text{-}OHO)][ClO_4]_7\cdot 2H_2O\cdot 3MeCN$ (**1**·3MeCN).

Fe(1)–O(1)	2.014(6)	Fe(3)–O(5)	2.022(6)
Fe(1)–O(3)	2.074(7)	Fe(3)–O(7)	2.048(6)
Fe(1)–O(9)	1.858(6)	Fe(3)–O(10)	1.980(6)
Fe(1)–O(12)	1.971(6)	Fe(3)–O(11)	1.873(6)
Fe(1)–N(1)	2.204(9)	Fe(3)–N(9)	2.224(9)
Fe(1)–N(5)	2.149(7)	Fe(3)–N(13)	2.168(7)
Fe(2)–O(2)	2.072(6)	Fe(4)–O(6)	2.029(6)
Fe(2)–O(4)	2.021(6)	Fe(4)–O(8)	2.028(5)
Fe(2)–O(9)	1.841(6)	Fe(4)–O(11)	1.882(6)
Fe(2)–O(10)	1.969(6)	Fe(4)–O(12)	1.942(6)
Fe(2)–N(4)	2.137(7)	Fe(4)–N(12)	2.161(7)
Fe(2)–N(8)	2.222(9)	Fe(4)–N(16)	2.221(8)
N(1)–Fe(1)–O(1)	75.9(3)	N(9)–Fe(3)–O(5)	75.6(3)
N(1)–Fe(1)–O(9)	173.2(3)	N(9)–Fe(3)–O(11)	170.0(3)
O(1)–Fe(1)–N(5)	158.4(3)	N(13)–Fe(3)–O(7)	76.5(2)
O(3)–Fe(1)–O(12)	168.6(3)	O(5)–Fe(3)–N(13)	161.0(3)
O(3)–Fe(1)–N(5)	76.8(3)	O(7)–Fe(3)–O(10)	166.7(2)
N(4)–Fe(2)–O(2)	76.1(3)	N(12)–Fe(4)–O(6)	75.0(3)
N(8)–Fe(2)–O(4)	75.1(3)	N(16)–Fe(4)–O(8)	75.8(3)
N(8)–Fe(2)–O(9)	171.9(3)	N(16)–Fe(4)–O(11)	169.5(3)
O(2)–Fe(2)–O(10)	165.9(3)	O(6)–Fe(4)–O(12)	164.5(3)
O(4)–Fe(2)–N(4)	159.6(3)	O(8)–Fe(4)–N(12)	160.6(3)
Fe(1)–O(9)–Fe(2)	149.2(4)	Fe(2)–O(10)–Fe(3)	133.0(3)
Fe(1)–O(12)–Fe(4)	132.8(3)	Fe(3)–O(11)–Fe(4)	150.3(4)

Table 2. Fe···Fe distances [Å] in tetranuclear iron(III) complexes having Fe–(OHO)–Fe bridging.

Structural type	Fe···Fe distances [Å]	Ref.
I	3.483(1), 3.566(1), 3.640(3), and 3.671(2)	[15e]
II (R = O)	3.397(2) and 3.755(2)	[15a]
II (R = Me)	3.451(1), 3.474(1), 3.675(1), and 3.709(1)	[15b,15c]
	3.440(2) and 3.7236(9); 3.4553(5) and 3.707(1)	[15d]
	3.424(1) and 3.704(1); 3.464(1), 3.485(1), and 3.730(1)	[15e]
II (R = $H_3NC_2H_4NH$)	3.336(1), 3.411(1), 3.677(1), and 3.730(1)	[15e]
III	3.250(2), 3.261(2), 3.687(2), and 3.694(2)	[15g,15h]
IV	3.561(1) and 3.625(1); 3.486(6), 3.581(6), 3.690(6), and 3.786(6)	[15e]
V	Fe(1)···Fe(2): 3.567(2), Fe(1)···Fe(4): 3.585(1);	this work
	Fe(2)···Fe(3): 3.622(1), Fe(3)···Fe(4): 3.630(2)	this work
VI	3.507, 3.575, 3.591, and 3.608	[15i]

and $\{Fe^{III}_4(\mu\text{-}RCO_2)_2(\mu\text{-}OHO)\}^{7+}$.[15i] The μ-oxido diiron(III) character in the Fe(1)–O(9)–Fe(2) and Fe(3)–O(11)–Fe(4) units is appreciably reduced as a result of an unsymmetrical protonation of the $\{O–H\cdots O\}^{3-}$ group. In essence, each of the Fe(1)/Fe(4) and Fe(2)/Fe(3) pairs is bridged by a single OH^- group and a $\{O–H\cdots O\}^{3-}$ group.

A compilation of Fe···Fe separations in **1**·3MeCN along with other Fe–(OHO)–Fe systems within the Fe_4O_4 family (Scheme 3) is provided in Table 2. A closer look at the metric parameters reveals that the four iron atoms in **1**·3MeCN are located at the vertices of a $\{Fe^{III}_4(\mu\text{-}OH)_2(\mu\text{-}OHO)\}^{7+}$ flattened tetragon (the average Fe–Fe–Fe angle within the Fe_4 core ≈ 85°), which is unique amongst all Fe–(OHO)–Fe bridged tetrairon(III) complexes reported so far (see below).

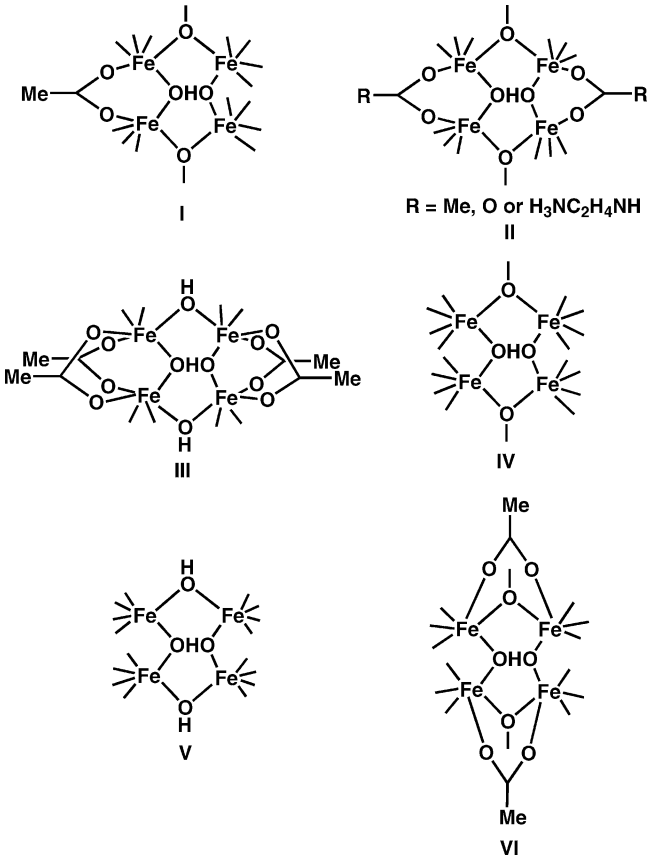

Scheme 3. Structural types of tetranuclear iron(III) complexes having Fe–(OHO)–Fe bridging.

Important structural parameters to consider in Fe–(OHO)–Fe bridged tetrairon(III) complexes are: (i) whether all iron atoms are in one plane, (ii) the coplanarity of bridging groups with the Fe_4 plane, and (iii) the coplanarity of the $\{OHO\}^{3-}$ bridging unit with the Fe_4 plane. Interestingly, for all reported systems, all four Fe atoms are exactly or almost exactly in the same plane (the displacements of oxygen atoms from the Fe_4 plane do not follow a regular trend; see Supporting Information). At variance, large deviations [Fe(1): 0.8803, Fe(2): –0.4246, Fe(3): 0.3965, and Fe(4): –0.4195 Å] are observed for **1**·3MeCN. The four oxygen atoms, however, form a plane with a deviation of ±0.0452 Å. Two iron atoms are above and two are below this plane by ±0.54 Å (Figure 1). As a result, **1**·3MeCN is the first example of a nonplanar Fe_4 core (tetragon) found in $\{Fe^{III}_4(\mu\text{-}OH)_2(\mu\text{-}OHO)\}^{7+}$ cluster chemistry.

At each iron site, one pyridyl nitrogen is *trans* to the $\{O–H\cdots O\}^{3-}$ unit, and the other one is *trans* to the amide oxygen, the former Fe–N bond being the longer because of the stronger *trans* effect of the $\{O–H\cdots O\}^{3-}$ group. At the Fe(1), Fe(2), and Fe(3) sites, the $Fe–O_{amide}$ bond *trans* to the hydroxy group is longer than the other one by ca. 0.06, ca. 0.05, and ca. 0.03 Å, respectively. Notably, at the Fe(4) site, the two $Fe–O_{amide}$ distances are comparable. Generally, the $Fe–N_{py}$ (py = pyridine) distances are longer than the $Fe–O_{amide}$ ones. At the Fe(1), Fe(2), Fe(3), and Fe(4) sites the differences are 0.13, 0.13, 0.16, and 0.16 Å, respectively. Clearly, the distortions are larger at the Fe(3) and Fe(4) than at the Fe(1) and Fe(2) sites.

Mössbauer Spectra

Mössbauer spectra of powdered samples of **1** have been recorded at 293, 80, and 4.5 K. All three spectra show (Figure 2) composite quadrupole-split doublets appearing as two very broad and asymmetric absorptions. No dipolar splitting due to internal magnetic field was observed even at very low temperature. As could be expected from these partly split absorptions it was not possible to fit the Mössbauer spectra of **1** by considering a unique quadrupole-split

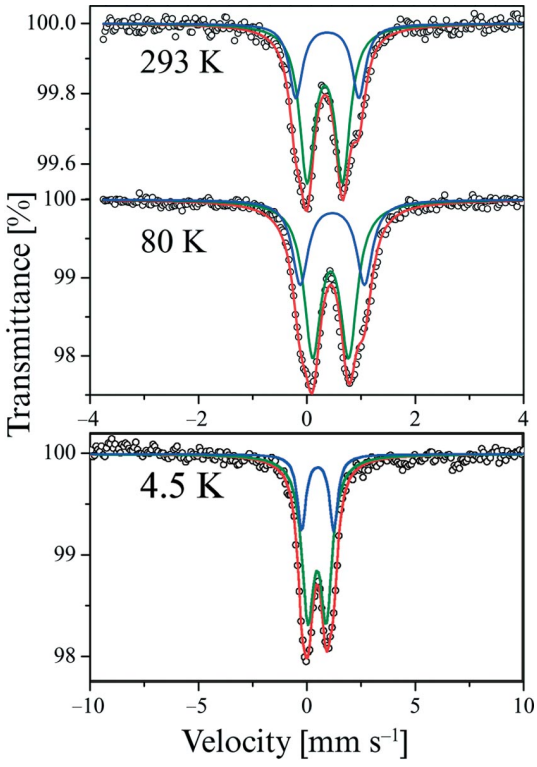

Figure 2. Mössbauer spectra of **1** (powdered sample) recorded in zero-field at 4.5 (lower trace), 80 (middle trace), and 293 K (top trace). The solid lines (blue and green for the minor and major sites, respectively, and red for the sum) represent the best least-squares fit to the experimental data (○).

doublet. In order to satisfactorily fit the spectra, it was necessary to consider two nested quadrupole-split doublets, i.e. of very close isomer shift (δ), in line with a very similar N_2O_4 environment for all four Fe sites, but significantly different quadrupole splittings (ΔE_Q). Two series of fittings were carried out, both yielding satisfactory results. For ligand environment and symmetry reasons discussed in the Crystal Structure section and below, the ferric sites may be associated by two Fe(1) and Fe(2) on one hand and Fe(3) and Fe(4) on the other hand. Consequently, we first constrained the area ratio of each doublet to 50%. Although the fit obtained was satisfactory, we were able to improve the fits by allowing for doublets with different area ratios. This resulted in minute variation of the δ and ΔE_Q parameters, while yielding unequal absorption areas of 70% and 30% in average. The data corresponding to these improved fits are shown in Figure 2 and collated in Table 3. Although the presence of two ferric doublets is not questionable, these fits are only indicative, i.e. no unambiguous site assignments can be achieved due to the overlap of the doublets and the small Mössbauer spectral parameter dependence on coordination environments for ferric sites.

The isomer shift values for the two sites are close to each other (δ = 0.44 and 0.47 mm s^{-1} at 80 K) and in agreement with related Fe^{III} (S = 5/2) sites.[15b–15d,15h,20b] The quadrupole splitting values are, however, very different (ΔE_Q = 0.67 mm s^{-1} and 1.19 mm s^{-1} at 80 K), clearly indicating quite different local symmetries at the two Fe^{III} sites[15b–15d,15h,20b,25] in spite of the similar N_2O_4 ligand en-

Table 3. Mössbauer spectral data for **1** and related Fe^{III}_4 clusters.[a]

Compound/Site(s)	Core/Bridges	T [K]	δ [mm s^{-1}][b]	ΔE_Q [mm s^{-1}]	$\Gamma_{1/2}$ [mm s^{-1}][c]	Area ratio [%]	Ref.
$[Fe_4(H_2bpp)_4(OH)_2(OHO)]^{7+}$	diamond[d]	4.5	0.493(11)	0.850(98)	0.339(36)	75(19)	this work
	(OHO)(OH)$_2$		0.521(18)	1.481(91)	0.231(71)	25(18)	
		80	0.4395(38)	0.666(16)	0.1881(88)	65.5(51)	
			0.4704(62)	1.186(25)	0.175(16)	34.5(53)	
		293	0.3319(51)	0.655(17)	0.166(10)	69.6(57)	
			0.3786(95)	1.163(29)	0.149(21)	30.4(60)	
$[Fe_4(dhpta)_2(O)(OH)(L\text{-ala})_2]^+$	rectangle	293	0.36	1.21	0.38	100	[15b,15c]
	(OHO)(OR)$_2$						
$[Fe_4(dhpta)(O)(OH)(O_2CMe)_2]^{3+}$	rectangle	293	0.36	1.15	0.37	100	[15d]
	(OHO)(OR)$_2$						
$[Fe_4(phen)_4(OHO)(OH)_2(O_2CMe)_4]^{3+}$	rectangle	80	0.470(1)	0.573(4)	0.144(2)	53.6(6)	
	(OHO)(OH)$_2$		0.485(2)	1.032(4)	0.144(2)	46.4(6)	[15g,15h]
		293	0.370(3)[e]	0.717(5)[e]	0.172(4)[e]	100[e]	
$[Fe_4(bpbp)_2(O)_2(OH)_2]^{4+}$	adamantane	4.5	0.490(1)	1.591(1)	0.138(1)	100	[26]
	(O)$_2$(OH)$_2$	80	0487(1)	1.601(2)	0.138(2)	100	
		293	0.383(2)	1.592(3)	0.137(2)	100	
$[Fe_4(hpba)_2(O_2CMe)_2(O)(OH)(OH_2)_2]^+$	tetragon	78	0.51(1)	0.58(1)	0.16(1)	25	[15i]
	(OHO)(OR)$_2$		0.51(1)	0.91(1)	0.16(1)	25	
			0.51(1)	1.14(1)	0.16(1)	25	
			0.51(1)	1.43(1)	0.16(1)	25	
		293	0.38(1)	0.78(1)	0.16(1)	50	
			0.38(1)	1.10(1)	0.16(1)	50	

[a] Ligand abbreviations: H_5dhpta = 1,3-diamino-2-hydroxypropane-*N*,*N*,*N*′,*N*′-tetracaetic acid; L-ala = L-alanine; phen = 1,10-phenanthroline; bpbp = 2,6-bis{[bis(2-picolyl)amino]methyl}-4-*tert*-butylphenol (Hbpbp); hpba = 2-[{2-hydroxy-5-methyl-3-[(pyridin-2-ylmethyl-amino)methyl]benzyl}(2-hydroxybenzyl)amino]acetic acid (H_3hpba). [b] Isomer shift relative to iron foil at room temperature. [c] Width at half height. [d] Core closer to distorted trapezium than to adamantane. [e] Data could not be fitted by two doublets because of the close proximity of the peaks.

vironments. The δ values decrease with increasing temperature because of the second-order Doppler effect. There is no significant thermal variation of the ΔE_Q values. It is thus clear that there are two different Fe^{III} (S = 5/2) sites in **1**: the difference in local symmetry of the ligand environments is large enough for allowing Mössbauer spectroscopy to easily distinguish two Fe sites.

This result is supported by the distortions evidenced in the single-crystal X-ray structure of **1**·3MeCN. While the bridges between Fe(1) and Fe(4), and Fe(2) and Fe(3), are identical (OH^- and $\{OHO\}^{3-}$), the unique bridge, $\{O(\cdots H-O)\}^{3-}$, between Fe(1) and Fe(2), is different from the bridge, $\{O(-H\cdots O)\}^{3-}$, between Fe(3) and Fe(4) (Figure 1). This difference in ligand environment between Fe(1) and Fe(2) on one hand and Fe(3) and Fe(4) on the other hand is corroborated by the Fe–O(H) distances: Fe(1)–O(9) and Fe(2)–O(9), 1.858(6) and 1.841(6) Å, respectively, are shorter than Fe(3)–O(11) and Fe(4)–O(11), which are 1.873(6) and 1.882(6) Å, respectively. Moreover, the Fe–O(H)–Fe angles [°] are equivalent by pairs: Fe(1)–O(9)–Fe(2) = 149.2(4), Fe(3)–O(11)–Fe(4) = 150.3(4) and Fe(1)–O(12)–Fe(4) = 132.8(3), Fe(2)–O(10)–Fe(3) = 133.0(3) (Table 1).

For purposes of comparison, the Mössbauer spectroscopic data of related tetranuclear iron(III) systems are also included in Table 3. From a structural viewpoint, the distorted "tetragonal" core of **1**·3MeCN (see above) resembles more a distorted "rectangular" than an "adamantane" core. Indeed, not only is there only one Fe site for the reported adamantane complex,[26] but its Mössbauer spectral parameters also differ significantly (Table 3). On the other hand, the data closer to those of the present Fe_4 complex are those of the distorted "rectangular" Fe_4 complex with similar bis(μ-OH){μ-(O···HO)} bridges (structural type III, Scheme 1),[15h] which, among the "rectangular" cores, has two Fe sites clearly distinguished by Mössbauer spectroscopy (ΔE_Q = 0.57 and 1.03 mm s^{-1}).

The larger ΔE_Q values for **1** (minor component) are notably smaller than those observed for μ-oxido dimers of Fe^{III},[20b,25] which may be ascribed to the less distorted octahedral coordination in **1**. The μ-oxido dimers have significantly shorter Fe–O_{oxido} bonds,[20–23] while the less distorted octahedral structure of Fe centers in **1** is associated to μ-OH and μ-(O–H···O)} bridges, at the exclusion of μ-oxido bridges.

Magnetic Properties

Magnetic susceptibility data of an analytically pure sample of **1** were measured by using a SQUID magnetometer. A plot of $\chi_M T$ (χ_M is the corrected molar magnetic susceptibility per tetramer) vs. temperature is displayed in Figure 3. The $\chi_M T$ value decreases gradually from 3.09 cm^3 mol^{-1} K at 300 K to a narrow plateau of 0.58 cm^3 mol^{-1} K at ca. 14 K, before reaching a value of 0.33 cm^3 mol^{-1} K at 2 K; the plateau, along with the non-zero value at 2 K, is the signature of a small amount of S = 5/2 paramagnetic impurity (see below). The room-temperature value of $\chi_M T$ for **1** is considerably less than that expected for four non-interacting Fe^{III} (S = 5/2) ions ($\chi_M T$ = 17.52 cm^3 mol^{-1} K for g = 2), indicating antiferromagnetic exchange interactions.

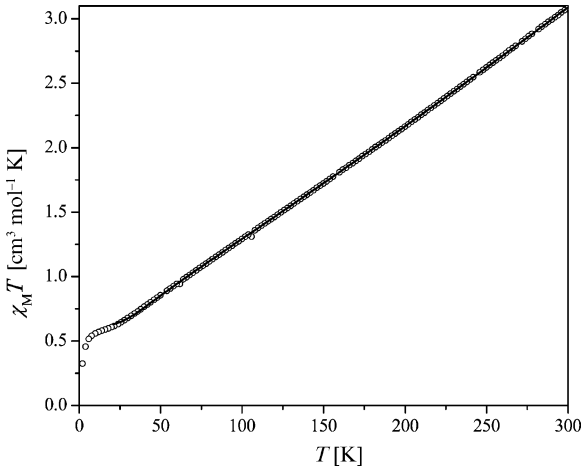

Figure 3. Temperature dependence of $\chi_M T$ for **1**. The solid line is a least-squares fit of the experimental data using the spin Hamiltonian described in the text.

Due to the lack of symmetry operations, six different exchange-coupling parameters should be considered for the interpretation of the magnetic properties of **1** (Scheme 4). However, due to the structural similarities of the Fe(1)–O(10)–Fe(2) and Fe(3)–O(12)–Fe(4) hydroxido interaction pathways, it is assumed that they can be accounted for by a single exchange-coupling parameter, i.e. $J_1 = J_{23} = J_{14}$. It is also assumed that the diagonal Fe(1)–O(9)···H(11)–O(11)–Fe(3) and Fe(2)–O(9)···H(11)–O(11)–Fe(4) pathways are inoperant. If we invoke that H(11) is mainly *localized* on O(11) and strongly hydrogen-bonded to O(9), i.e. weakly delocalized towards O(9) (see description of the structure), then this should induce different degrees of hydroxido character on each oxido. Therefore, taking into account that oxido bridges provide stronger antiferromagnetic interaction than hydroxido bridges, we consider that the Fe(1)···Fe(2) magnetic interaction (J_2) should be different from the Fe(3)···Fe(4) interaction (J_3). The magnetic exchange coupling model taking into account these structural characteristics is presented in Scheme 3; the corresponding exchange Hamiltonian considered including a zero-field splitting (zfs) term D common for the four iron sites ($D_1 = D_2 = D_3 = D_4 = D$) is given in Equation (2).

$$\hat{H} = -2\left[J_1(\hat{S}_1\hat{S}_4 + \hat{S}_2\hat{S}_3) + J_2\hat{S}_1\hat{S}_2 + J_3\hat{S}_3\hat{S}_4\right] + D(\hat{S}_{z_1}^2 + \hat{S}_{z2}^2 + \hat{S}_{z3}^2 + \hat{S}_{z4}^2) \quad (2)$$

The magnetic susceptibility has been computed by exact calculation of the energy levels associated to this spin Hamiltonian through diagonalization of the full-matrix with a general program for axial symmetry.[27] Least-squares fittings were accomplished with an adapted version of the function-minimization program MINUIT.[28] Comparison

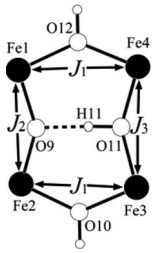

Scheme 4. The model used for interpreting the magnetic data of **1**.

of different fits carried out by setting D to zero or g to 2 show that the J_1, J_2, and J_3 values and the quality of the fits are very weakly affected upon setting D to zero and g to 2. Thus, in order to avoid over-parametrization, the zfs parameter D was set to zero and g was set to 2 in the final fits. While the data above ca. 20 K were very nicely fitted with this coupling model (Figure 3), the presence of a small fraction of paramagnetic impurity precluded fitting the data below 20 K, possibly because of the zero-field splitting of this paramagnetic component. Exploration of the parameter space of the problem revealed two local minima, with best-fit parameters: $J_1 = -30.9\ cm^{-1}$, $J_2 = -96.4\ cm^{-1}$, $J_3 = -34.7\ cm^{-1}$, $g = 2$ (fixed), ρ [molar percentage of mononuclear Fe^{III} ($S = 5/2$) paramagnetic impurity] = 1.77%, with $R = 1.9 \times 10^{-5}$ (solution A) and $J_1 = -44.7\ cm^{-1}$, $J_2 = -62.8\ cm^{-1}$, $J_3 = -26.2\ cm^{-1}$, $g = 2$ (fixed), $\rho = 1.76\%$, with $R = 1.9 \times 10^{-5}$ (solution B). Since J_1 refers to hydroxido-mediated exchange coupling, J_3 to a dominantly hydroxido-mediated exchange coupling, and J_2 to a dominantly oxido-mediated exchange coupling, we expect that $|J_1| < |J_3| < |J_2|$. Thus we rule out solution B on the basis of its lack of physical meaning, since it is characterized by $|J_3| < |J_1| < |J_2|$. Indeed, in solution B, not only are the purely hydroxido-mediated interactions (J_1) too strong and the dominantly oxido-mediated one (J_2) too weak, but also, in spite of its partial oxido character, $|J_3| < |J_1|$, whereas the opposite effect is expected. The best fit corresponding to solution A is displayed in Figure 3. As the J_1 and J_3 values of solution A are close to each other, we also considered the possibility to fit the magnetic data of **1** to a two-J model ($J_1 \approx J_3$). However, these attempts did not yield any acceptable fit.

The observed J values for **1**, structural parameters, and coupling constants for closely related complexes are collated in Table 4. Given the molecular structure of **1**·3MeCN and the model used, the calculated values of J_1, J_2, and J_3 are reasonable (Table 4). Relative to closely similar reported complexes,[15g,15h] the increase in the extent of antiferromagnetic coupling in **1** may be due to a lowering of the effective core symmetry,[29] because of the unsupported nature of the $\{Fe_4(\mu\text{-}OH)_2\{\mu\text{-}(O\text{–}H\cdots O)\}^{7+}$ core in **1**, facilitating more symmetry-allowed overlap of metal d orbitals with p orbitals of hydroxido and $(OHO)^{3-}$ bridges. To the best of our knowledge, this is the second time that three exchange interactions have been considered to fit experimental data for a $\{\mu\text{-}(O\text{–}H\cdots O)\}^{3-}$ bridged Fe_4 core. Amongst the $(OHO)^{3-}$ bridged tetrairon(III) complexes reported so far, the $[\{Fe_2(OR')(RCO_2)\}_2(OHO)]^{1+}$ cation[15i] was the first to exhibit different enough degrees of hydroxido character on each oxido for mediating three different magnetic exchange interactions. It is also worth noting here that theoretical calculations at the density functional theory level have been carried out very recently for Fe_4O_4 "butterfly" cores by considering three magnetic exchange interactions.[30]

Table 4. Structural parameters and magnetic exchange coupling constant (J) values for Fe–(OHO)–Fe bridged tetranuclear iron(III) complexes.

Structural type	Fe–O(H) distance [Å]	Fe–O–Fe angle [°]	J [cm^{-1}]	Ref.
II (R = O)	Fe_2(μ-alkoxido): Av. 2.053(4) Fe_2(μ-OHO): 1.829(4)	Fe–(O–alkoxido)–Fe: 132.3(2) Fe–(OHO)–Fe: 136.4(3)	Fe–(μ-alkoxido)–Fe: –11 Fe-(μ-OHO)(μ-OCO_2)–Fe: –63	[15a]
II (R = Me)	Fe_2(μ-alkoxido): Av. 2.019(4) Fe_2(μ-OHO): 1.853(4), 1.862(4), 1.850(4), 1.850(4)	Fe–(O–alkoxido)–Fe: Av. 132.2(2) Fe–(OHO)–Fe: Av. 138.1(3)	Fe–(μ-alkoxido)–Fe: – 21 Fe–(μ-OHO)(μ-O_2CMe)–Fe: –42	[15b,c]
III	Fe–(μ-OH): 1.997(7), 1.997(7), 1.984(7), 2.002(7) Fe_2(μ-OHO): 1.883(6), 1.869(6), 1.881(7), 1.876(7)	Fe–(OH)–Fe: 135.3(4), 135.3(4) Fe–(OHO)–Fe: 120.7(4), 119.8(4)	Fe–(μ-OH)–Fe: –22 Fe–(μ-OHO)(μ-O_2CMe)$_2$–Fe: –74	[15g,h]
IV	Fe_2(μ-alkoxido): Av. 1.997(3) Fe_2(μ-OHO): 1.864(4)	Fe–(O–alkoxido)-Fe: 130.65(2) Fe–(OHO)–Fe: 145.65(2)	Fe–(μ-alkoxido)–Fe: –14 Fe–(μ-OHO)–Fe: –34	[15f]
V	Fe–(μ-OH): 1.942(6), 1.971(6), 1.969(6), 1.980(6) within Fe_2(μ-OHO) unit: Fe–(μ-O): 1.841(6), 1.858(6) Fe–(μ-OH): 1.873(6), 1.882(6)	Fe–(OH)–Fe: 132.8(3), 133.0(3) within Fe–(OHO)–Fe unit: Fe–(O)–Fe: 149.3(4) Fe–(OH)–Fe: 150.4(4)	Fe–(μ-OH)–Fe: –31 within Fe–(μ-OHO)–Fe unit: Fe–(μ-O)–Fe: –96 Fe–(μ-OH)–Fe: –35	this work
VI	Fe_2(μ-phenoxido): Av. 2.061(4) within Fe_2(μ-OHO) unit: Fe–(μ-O): 1.841(4), 1.819(4) Fe–(μ-OH): 1.884(4), 1.909(4)	Fe_2(μ-phenoxido): Av. 120.76(17) within Fe–(OHO)–Fe unit: Fe–(μ-O)–Fe: 146.8(2) Fe–(μ-OH)–Fe: 144.0(2)	Fe–(μ-phenoxido)–Fe: –29 within Fe–(μ-OHO)–Fe unit: Fe–(μ-O)–Fe: –40 Fe–(μ-OH)–Fe: –13	[15i]

Concluding Remarks

From the X-ray structural results for **1**·3MeCN presented here, it appears that neutral bis(2-pyridinecarboxamide) ligands with alkane spacers have appreciable propensity for linking metal ions into polymetallic networks, in the present case a discrete tetrairon(III) complex. It should be kept in mind that the amide group, a key component of proteins, also participates in binding metal ions in mononuclear non-heme iron proteins.[31] The present work is an extension of our efforts to demonstrate efficient coordination of amide oxygen towards transition-metal ions[13a] to synthesize discrete molecules and to eventually provide suitable bioinspired synthetic models. The "tetragonal" $[Fe_4(\mu\text{-}OH)_2\{\mu\text{-}(O\text{–}H\cdots O)\}]^{7+}$ core present in **1**·3MeCN, assembled without use of an endogenous bridging ligand and/or carboxylate bridges, qualifies as an unprecedented example of the tetrairon(III) family bridged solely by two hydroxido ligands and an O–H···O bridging unit. It is a valuable addition to the coordination chemistry of tetrairon(III) clusters in general and bioinorganic chemistry in particular. Furthermore, the strongly hydrogen-bonded $\{O\text{–}H\cdots O\}^{3-}$ bridge could provide useful structural information in relation to the mechanism of water oxidation in photosystem II, which involves a tetramanganese core, and its synthetic and theoretical studies.[32] Efforts to understand the generality of this core formation are continuing.

Experimental Section

General: All reagents were obtained from commercial sources and used as received, unless stated otherwise. Solvents were dried/purified as reported previously.[2,6] The ligand H_2bpp[11] and $[Fe(MeCN)_4][ClO_4]_2$[14] were prepared by following reported procedures.

Synthesis of $[Fe_4(H_2bpp)_4(\mu\text{-}OH)_2(\mu\text{-}OHO)][ClO_4]_7\cdot 2H_2O\cdot x$MeCN ($1\cdot x$MeCN, $0 \le x \le 3$): To a stirred solution of H_2bpp (0.07 g, 0.24 mmol) in MeCN (4 mL) was added solid $[Fe(MeCN)_4][ClO_4]_2$ (0.1 g, 0.24 mmol) portionwise. The reddish-orange solution thus formed was stirred in air for 2 h at 298 K. Ethyl acetate (5 mL) was added, yielding a reddish-brown gummy mass. The mass was dissolved in acetone (15 mL) by continuous stirring and 2-propanol (20 mL) was added. The resulting solution was kept at 298 K for 2 d. The crystalline orange precipitate that resulted was filtered, washed with 2-propanol, and dried in vacuo. Yield: 0.075 g (53%). Single crystals of **1**·3MeCN were obtained by vapor diffusion of diethyl ether into a MeCN solution of the complex. Notably, the crystals thus obtained rapidly lose solvent. **1**·3MeCN ($C_{66}H_{80}Cl_7Fe_4N_{19}O_{42}$): calcd. C 34.72, H 3.53, N 11.66; found C 34.78, H 3.24, N 11.69. IR (KBr disc; selected peaks): $\tilde{\nu}$ = 3410 and 3072 [ν(OH)], 3340 [ν(NH)], 1640 [amide I; mainly ν(CO)] and 1555 [amide II; mainly ν(CN)], 1086 [$\nu(ClO_4^-)$] cm^{-1}. UV/Vis (MeCN): λ (ε, $M^{-1}\,cm^{-1}$) = 265 (74600), 360 (14400) nm. UV/Vis (MeOH): λ (ε, $M^{-1}\,cm^{-1}$) = 260 (65 000), 330 sh (12000) nm.

Caution: Perchlorate complexes are potentially explosive and should be handled with care. However, the small quantities used in our studies did not pose a hazard.

Physical Measurements: Elemental analyses were obtained with a Carlo Erba CHNSO 1110 analyzer. Spectroscopic measurements were made by using the following instruments: IR (KBr, 4000–600 cm^{-1}): Bruker Vector 22; UV/Vis: Perkin–Elmer Lambda 2 and Agilent 8453 diode-array spectrophotometers.

Mössbauer Spectra: Mössbauer spectra were recorded with a constant-acceleration conventional spectrometer with a 50 mCi source of ^{57}Co (Rh matrix). The absorber was a powdered sample enclosed in a cylindrical plastic sample holder of 20 mm diameter, the size of which was determined to optimize the absorption. Spectra were obtained in the 4–300 K range by using a MD306 Oxford cryostat, the thermal scanning being monitored by an Oxford ITC4 servo control device (accuracy: ±0.1 K). A least-squares computer program[33] was used to fit the Mössbauer spectral parameters and to determine their standard deviations of statistical origin (given in parentheses). Isomer shift values (δ) are relative to iron foil at 293 K.

Magnetism: Variable temperature magnetic susceptibility data (5–300 K) were collected for powdered samples with a MPMS-55 Quantum Design SQUID magnetometer in the sweeping mode (1 K min^{-1}) under an applied magnetic field of 1 T. Diamagnetic corrections were applied by using Pascal's constants.

Crystallography: X-ray data were collected with a Bruker SMART APEX CCD diffractometer, with graphite-monochromated Mo-K_α (λ = 0.71073 Å) radiation at 100(2) K. The "Bruker Saint Plus" program[34] was used for data reduction. Data were corrected for Lorentz and polarization effects; an empirical absorption correction (SADABS) was applied.[35] The structure was solved by direct methods with SIR-97 and refined by full-matrix least-squares methods based on F^2 by using SHELXL-97, incorporated in the WinGX 1.64 crystallographic package.[36] All non-hydrogen atoms were refined with anisotropic thermal parameters. The positions of the hydrogen atoms were calculated assuming ideal geometries, but not refined. The hydrogen atoms of water molecules could not be located or fixed satisfactorily. A summary of the data collection and structure refinement information is provided in Table 5. The high values for R and R_w are due to the poor quality of the crystals, resulting from partial solvent loss, and to the lack of high-angle scattering.

Table 5. Crystallographic data for $[Fe_4(H_2bpp)_4(\mu\text{-}OH)_2(\mu\text{-}OHO)](ClO_4)_7\cdot 2H_2O\cdot 3$MeCN (**1**·3MeCN).

Molecular formula	$C_{66}H_{80}Cl_7N_{19}O_{42}Fe_4$
M_r	2283.02
Temperature [K]	100(2)
Crystal system	orthorhombic
Space group	*Fdd*2 (no. 43)
a [Å]	46.484(5)
b [Å]	54.222(5)
c [Å]	14.975(5)
V [Å^3]	37744(14)
Z	16
D_c [g cm^{-3}]	1.596
λ [Å]	0.71073
μ [mm^{-1}]	0.901
Reflections measured	62954
Unique reflections, R_{int}	22902, 0.0945
Observed reflections [$I > 2\sigma(I)$]	15349
Refined parameters	1243
R[a] (R_w)[b]	0.1106 (0.2420)
R[a] (R_w)[b] (all data)	0.1528 (0.2669)
Goodness-of-fit on F^2	1.067

[a] $R_1 = \Sigma(|F_o| - |F_c|)/\Sigma|F_o|$. [b] $wR_2 = \{\Sigma[w(|F_o|^2 - |F_c|^2)^2]/\Sigma[w(|F_o|^2)^2]\}^{1/2}$.

CCDC-668588 contains the supplementary crystallographic data for **1**·3MeCN. These data can be obtained free of charge from the Cambridge Crystallographic Data Centre via www.ccdc.cam.ac.uk/data_request/cif.

Supporting Information (see also the footnote on the first page of this article): IR spectrum and UV/Vis spectra in MeCN and MeOH for **1**.

Acknowledgments

We thank the Council of Scientific & Industrial Research and the Department of Science and Technology, Government of India, New Delhi for financial support.

[1] O. Belda, C. Moberg, *Coord. Chem. Rev.* **2005**, *249*, 727–740.
[2] a) A. K. Singh, R. Mukherjee, *Dalton Trans.* **2008**, 260–270; b) A. K. Singh, R. Mukherjee, *Inorg. Chem.* **2005**, *44*, 5813–5819; c) A. K. Singh, R. Mukherjee, *Dalton Trans.* **2005**, 2886–2891; d) A. K. Patra, M. Ray, R. Mukherjee, *Inorg. Chem.* **2000**, *39*, 652–657; e) A. K. Patra, M. Ray, R. Mukherjee, *J. Chem. Soc., Dalton Trans.* **1999**, 2461–2466; f) A. K. Patra, R. Mukherjee, *Polyhedron* **1999**, *18*, 1317–1322.
[3] a) K. Ghosh, A. A. Eroy-Reveles, M. M. Olmstead, P. K. Mascharak, *Inorg. Chem.* **2005**, *44*, 8469–8475; b) A. K. Patra, M. J. Rose, M. M. Olmstead, P. K. Mascharak, *J. Am. Chem. Soc.* **2004**, *126*, 4780–4781; c) D. S. Marlin, M. M. Olmstead, P. K. Mascharak, *Eur. J. Inorg. Chem.* **2002**, 859–865; d) J. M. Rowland, M. M. Olmstead, P. K. Mascharak, *Inorg. Chem.* **2000**, *39*, 5326–5332; e) L. A. Tyler, J. C. Noveron, M. M. Olmstead, P. K. Mascharak, *Inorg. Chem.* **2000**, *39*, 357–362.
[4] a) A. Mohamadou, J.-P. Barbier, J. Marrot, *Inorg. Chim. Acta* **2007**, *360*, 2485–2491; b) S. Hubert, A. Mohamadou, C. Gérard, J. Marrot, *Inorg. Chim. Acta* **2007**, *360*, 1702–1710; c) S. Nag, R. J. Butcher, S. Bhattacharya, *Eur. J. Inorg. Chem.* **2007**, 1251–1260; d) C. F. Fortney, S. J. Geib, F.-t. Lin, R. E. Shepherd, *Inorg. Chim. Acta* **2005**, *358*, 2921–2932; e) J. M. Domínguez-Vera, J. Suárez-Varela, I. B. Maimoun, E. Colacio, *Eur. J. Inorg. Chem.* **2005**, 1907–1912; f) C. F. Fortney, R. E. Shepherd, *Inorg. Chem. Comun.* **2004**, *7*, 1065–1070; g) A. Das, S.-M. Peng, G.-H. Lee, S. Bhattacharya, *New J. Chem.* **2004**, *28*, 712–717; h) J.-Y. Qi, Q.-Y. Yang, S.-S. Chan, Z.-Y. Zhou, A. S. C. Chan, *Acta Crystallogr., Sect. C* **2004**, *60*, m210–m211; i) J.-Y. Qi, H.-X. Ma, X.-J. Li, Z.-Y. Zhou, M. C. K. Choi, A. S. C. Chan, Q.-Y. Yang, *Chem. Commun.* **2003**, 1294–1295; j) J.-Y. Qi, L. Q. Qiu, K. H. Lam, C. W. Yip, Z. Y. Zhou, A. S. C. Chan, *Chem. Commun.* **2003**, 1058–1059; k) C. Jubert, A. Mohamadou, C. Gérard, S. Brandes, A. Tabard, J.-P. Barbier, *J. Chem. Soc., Dalton Trans.* **2002**, 2660–2669; l) M. Amirnasr, K. J. Schenk, S. Meghdadi, *Inorg. Chim. Acta* **2002**, *338*, 19–26.
[5] a) U. Beckmann, E. Bill, T. Weyhermüller, K. Wieghardt, *Inorg. Chem.* **2003**, *42*, 1045–1056; b) S. K. Dutta, U. Beckmann, E. Bill, T. Weyhermüller, K. Wieghardt, *Inorg. Chem.* **2000**, *39*, 3355–3364.
[6] a) A. K. Singh, V. Balamurugan, R. Mukherjee, *Inorg. Chem.* **2003**, *42*, 6497–6502; b) A. K. Patra, M. Ray, R. Mukherjee, *Polyhedron* **2000**, *19*, 1423–1428; c) A. K. Patra, R. Mukherjee, *Inorg. Chem.* **1999**, *38*, 1388–1393; d) M. Ray, D. Ghosh, Z. Shirin, R. Mukherjee, *Inorg. Chem.* **1997**, *36*, 3568–3572.
[7] a) T. C. Harrop, L. A. Tyler, M. M. Olmstead, P. K. Mascharak, *Eur. J. Inorg. Chem.* **2003**, 475–481; b) D. S. Marlin, M. M. Olmstead, P. K. Mascharak, *Eur. J. Inorg. Chem.* **2002**, 859–865; c) J. C. Noveron, M. M. Olmstead, P. K. Mascharak, *J. Am. Chem. Soc.* **2001**, *123*, 3247–3259; d) L. A. Tyler, M. M. Olmstead, P. K. Mascharak, *Inorg. Chim. Acta* **2001**, *321*, 135–141; e) J. C. Noveron, M. M. Olmstead, P. K. Mascharak, *J. Am. Chem. Soc.* **1999**, *121*, 3553–3554.
[8] a) I. V. Korendovych, O. P. Kryatova, W. M. Reiff, E. V. Rybak-Akimova, *Inorg. Chem.* **2007**, *46*, 4197–4211; b) I. V. Korendovych, R. J. Staples, W. M. Reiff, E. V. Rybak-Akimova, *Inorg. Chem.* **2004**, *43*, 3930–3941; c) S. L. Jain, P. Bhattacharya, H. L. Milton, A. M. Z. Slawin, J. A. Crayston, J. D. Woolins, *Dalton Trans.* **2004**, 862–871; d) E. Kolomiets, V. Berl, I. Odriozola, A.-M. Stadler, N. Kyritsakas, J.-M. Lehn, *Chem. Commun.* **2003**, 2868–2869; e) Z. Shirin, J. Thompson, L. Liable-Sands, G. P. A. Yap, A. L. Rheingold, A. S. Borovik, *J. Chem. Soc., Dalton Trans.* **2002**, 1714–1720; f) T. Yano, R. Tanaka, T. Nishioka, I. Kinoshita, K. Isobe, L. J. Wright, T. J. Collins, *Chem. Commun.* **2002**, 1396–1397.
[9] a) P. K. Mascharak, *Coord. Chem. Rev.* **2002**, *225*, 201–214; b) T. C. Harrop, P. K. Mascharak, *Acc. Chem. Res.* **2004**, *37*, 253–260; c) J. A. Kovacs, *Chem. Rev.* **2004**, *104*, 825–848.
[10] a) B. M. Trost, K. Dogra, I. Hachiya, T. Emura, D. L. Hughes, S. Krska, R. A. Reamer, M. Palucki, N. Yasuda, P. J. Reider, *Angew. Chem. Int. Ed.* **2002**, *41*, 1929–1932; b) D. A. Conlon, N. Yasuda, *Adv. Synth. Catal.* **2001**, *343*, 137–138.
[11] D. J. Barnes, R. L. Chapman, R. S. Vagg, E. C. Watton, *J. Chem. Eng. Data* **1978**, *23*, 349–350.
[12] a) S. Tsuboyama, T. Sakurai, K. Kobayashi, N. Azuma, Y. Kajikawa, K. Ishizu, *Acta Crystallogr., Sect. B* **1984**, *40*, 466–473; b) Y. Kajikawa, T. Sakurai, N. Azuma, S. Kohno, S. Tsuboyama, K. Kobayashi, K. Mukai, K. Ishizu, *Bull. Chem. Soc. Jpn.* **1984**, *57*, 1454–1458; c) Y. Kajikawa, N. Azuma, K. Tajima, *Inorg. Chim. Acta* **1998**, *283*, 61–71; d) C. F. Fortney, S. J. Geib, F.-t. Lin, R. E. Shepherd, *Inorg. Chim. Acta* **2005**, *358*, 2921–2932.
[13] a) W. Jacob, R. Mukherjee, *Inorg. Chim. Acta* **2006**, *359*, 4565–4573 and references cited therein; b) C. R. Cornman, E. P. Zovinka, Y. D. Boyajian, M. M. Olmstead, B. C. Noll, *Inorg. Chim. Acta* **1999**, *285*, 134–137.
[14] S. A. Richert, P. K. S. Tsang, D. T. Sawyer, *Inorg. Chem.* **1989**, *28*, 2471–2475.
[15] Tetragon-type Fe_4O_4 core: a) D. L. Jameson, C.-L. Xie, D. N. Hendrickson, J. A. Potenza, H. J. Schugar, *J. Am. Chem. Soc.* **1987**, *109*, 740–746; b) S. Yano, T. Inagaki, Y. Yamada, M. Kato, M. Yamasaki, K. Sakai, T. Tsubomura, M. Sato, W. Mori, K. Yamaguchi, I. Kinoshita, *Chem. Lett.* **1996**, 61–62; c) T. Tanase, T. Inagaki, Y. Yamada, M. Kato, E. Ota, M. Yamazaki, M. Sato, W. Mori, K. Yamaguchi, M. Mikuriya, M. Takahashi, M. Takeda, I. Kinoshita, S. Yano, *J. Chem. Soc., Dalton Trans.* **1998**, 713–718; d) T. Tanase, C. Inoue, S. Yano, M. Takahashi, M. Takeda, *Inorg. Chim. Acta* **2000**, *297*, 18–26; e) W. Schmitt, C. E. Anson, R. Sassoli, M. van Veen, A. K. Powell, *J. Inorg. Biochem.* **2002**, *91*, 173–189; f) W. Schmitt, C. E. Anson, B. Pilawa, A. K. Powell, *Z. Anorg. Allg. Chem.* **2002**, *628*, 2443–2457; g) A. K. Boudalis, N. Lalioti, G. A. Spyroulias, C. P. Raptopoulou, A. Terzis, V. Tangoulis, S. P. Perlepes, *J. Chem. Soc., Dalton Trans.* **2001**, 955–957; h) A. K. Boudalis, N. Lalioti, G. A. Spyroulias, C. P. Raptopoulou, A. Terzis, A. Bousseksou, V. Tangoulis, J.-P. Tuchagues, S. P. Perlepes, *Inorg. Chem.* **2002**, *41*, 6474–6487; i) A. K. Boudalis, R. E. Aston, S. J. Smith, R. E. Mirams, M. J. Riley, G. Schenk, A. G. Blackman, L. R. Hanton, L. R. Gahan, *Dalton Trans.* **2007**, 5132–5139.
[16] Dimer-of-dimer type Fe_4O_4 core: a) Q. Chen, J. B. Lynch, P. Gomez-Romero, A. Ben-Hussein, G. B. Jameson, C. J. O'Connor, L. Que Jr, *Inorg. Chem.* **1988**, *27*, 2673–2681; b) J. H. Satcher Jr, M. M. Olmstead, M. W. Droege, S. R. Parkin, B. C. Noll, L. May, A. L. Balch, *Inorg. Chem.* **1998**, *37*, 6751–6758; c) A. Horn, A. Neves, A. J. Bortoluzzi, V. Drago, W. A. Ortiz, *Inorg. Chem. Commun.* **2001**, *4*, 173–176.
[17] By using a variety of ligand systems, the following structural types have also been synthesized: (i) dimer-of-dimer $\{Fe_2(O)(RCO_2)_2\}^{2+}$, (ii) butterfly ($Fe_4O_2$), (iii) tetrahedral ($Fe_4O_2$), (iv) cubane ($Fe_4O_4$), (iv) adamantane ($Fe_4O_6$), and (vi) face-to-face $[\{Fe_2(OR')_2(RCO_2)\}_2(O)_2]^{2+}$ (OR′: phenolato). The list of references is given in the Supporting Information.

[18] D. S. Marlin, P. K. Mascharak, *Chem. Soc. Rev.* **2000**, *29*, 69–74.
[19] a) P. Chaudhuri, K. Wieghardt, B. Nuber, J. Weiss, *Angew. Chem. Int. Ed. Engl.* **1985**, *24*, 778–779; b) W. H. Armstrong, S. J. Lippard, *J. Am. Chem. Soc.* **1984**, *106*, 4632–4633.
[20] a) B. O. West, *Polyhedron* **1989**, *8*, 219–274; b) D. M. Kurtz Jr, *Chem. Rev.* **1990**, *90*, 585–606.
[21] a) K. Wieghardt, K. Pohl, W. Gebert, *Angew. Chem. Int. Ed. Engl.* **1983**, *22*, 727; b) W. H. Armstrong, S. J. Lippard, *J. Am. Chem. Soc.* **1983**, *105*, 4837–4838; c) W. H. Armstrong, A. Spool, G. C. Papaefthymiou, R. B. Frankel, S. J. Lippard, *J. Am. Chem. Soc.* **1984**, *106*, 3653–3667; d) J. R. Hartman, R. L. Rardin, P. Chaudhuri, K. Pohl, K. Wieghardt, B. Nuber, J. Weiss, G. C. Papaefthymiou, R. B. Frankel, S. J. Lippard, *J. Am. Chem. Soc.* **1987**, *109*, 7387–7396; e) K. L. Taft, A. Masschelein, S. Liu, S. J. Lippard, D. Garfinkel-Shweky, A. Bino, *Inorg. Chim. Acta* **1992**, *198–200*, 627–631; f) K. B. Jensen, C. J. McKenzie, O. Simonsen, H. Toftlund, A. Hazell, *Inorg. Chim. Acta* **1997**, *257*, 163–172; g) T. J. Mizoguchi, R. M. Davydov, S. J. Lippard, *Inorg. Chem.* **1999**, *38*, 4098–4103.
[22] R. Mukherjee, T. D. P. Stack, R. H. Holm, *J. Am. Chem. Soc.* **1988**, *110*, 1850–1861.
[23] J. Mukherjee, V. Balamurugan, R. Gupta, R. Mukherjee, *Dalton Trans.* **2003**, 3686–3692.
[24] a) G. A. Jeffrey, *An Introduction to Hydrogen Bonding*, Oxford, New York, **1997**; b) D. Braga, A. Angeloni, E. Tagliavini, F. Grepioni, *J. Chem. Soc., Dalton Trans.* **1998**, 1961–1968.
[25] E. Y. Tshuva, S. J. Lippard, *Chem. Rev.* **2004**, *104*, 987–1012.
[26] M. Ghiladi, F. B. Larsen, C. J. McKenzie, I. Søtofte, J.-P. Tuchagues, *Dalton Trans.* **2005**, 1687–1692.
[27] a) J. Aussoleil, P. Cassoux, P. de Loth, J.-P. Tuchagues, *Inorg. Chem.* **1989**, *28*, 3051–3056; b) J. M. Clemente-Juan, C. Mackiewicz, M. Verelst, F. Dahan, A. Bousseksou, Y. Sanakis, J.-P. Tuchagues, *Inorg. Chem.* **2002**, *41*, 1478–1491.
[28] "*MINUIT Program, a System for Function Minimization and Analysis of the Parameter Errors and Correlations*": F. James, M. Roos, *Comput. Phys. Commun.* **1975**, *10*, 343–367.
[29] P. Gomez-Romero, E. H. Witten, W. M. Reiff, G. B. Jameson, *Inorg. Chem.* **1990**, *29*, 5211–5217.
[30] T. Cauchy, E. Ruiz, S. Alvarez, *J. Am. Chem. Soc.* **2006**, *128*, 15722–15727.
[31] a) A. L. Feig, S. J. Lippard, *Chem. Rev.* **1994**, *94*, 759–806; b) L. Que Jr, R. Y. N. Ho, *Chem. Rev.* **1996**, *96*, 2607–2624.
[32] J. P. McEvoy, G. W. Brudvig, *Chem. Rev.* **2006**, *106*, 4455–4483.
[33] K. Lagarec, *Recoil, Mössbauer Analysis Software for Windows*, http://www.physics.uottawa.ca/~recoil
[34] *SAINT Plus, Software for CCD Diffractometers*, Bruker AXS, Madison, WI, USA, **2000**.
[35] *SADABS, Program for Correction of Area Detector Data*, Universität Göttingen, Göttingen, Germany, **1999**.
[36] L. J. Farrugia, *WinGX, An Integrated System of Windows Programs for the Solution, Refinement and Analysis of Single-Crystal X-ray Diffraction Data*, version 1.64, Department of Chemistry, University of Glasgow, **2003**.

Received: January 12, 2008
Published Online: May 13, 2008

